Organic Electronics 15 (2014) 3492–3500

Contents lists available at ScienceDirect

Organic Electronics

journal homepage: www.elsevier.com/locate/orgel

Silver grid transparent conducting electrodes for organic light emitting diodes

F. Laurent M. Sam, M. Anas Razali, K.D.G. Imalka Jayawardena, Christopher A. Mills, Lynn J. Rozanski, Michail J. Beliatis, S. Ravi P. Silva *

Advanced Technology Institute, Department of Electronic Engineering, University of Surrey, Guildford, Surrey GU2 7XH, UK

ARTICLE INFO

Article history:
Received 11 June 2014
Received in revised form 28 July 2014
Accepted 24 September 2014
Available online 11 October 2014

Keywords:
Metal grids
Transparent conducting electrodes
ITO alternatives
OLEDs

ABSTRACT

Polymer organic light emitting diodes (OLEDs) were fabricated using thin silver hexagonal grids replacing indium tin oxide (ITO) as the transparent conducting electrodes (TCE). Previous literature has assumed that thick metal grids (several hundred nanometres thick) with a lower sheet resistance (<10 Ω/□) and a similar light transmission (>80%) compared to thinner grids would lead to OLEDs with better performance than when thinner metal grid lines are used. This assumption is critically examined using OLEDs on various metal grids with different thicknesses and studying their performances. The experimental results show that a 20 nm thick silver grid TCE resulted in more efficient OLEDs with higher luminance (10 cd/A and 1460 cd/m^2 at 6.5 V) than a 111 nm thick silver grid TCE (5 cd/A and 159 cd/m^2 at 6.5 V). Furthermore, the 20 nm thick silver grid OLED has a higher luminous efficiency than the ITO OLED (6 cd/A and 1540 cd/m^2 at 6.5 V) at low voltages. The data shows that thinner metal grid TCEs (about 20 nm) make the most efficient OLEDs, contrary to previous expectations.

1. Introduction

Transparent conducting electrodes (TCEs) are an important component in organic light emitting diodes (OLEDs). They allow the efficient extraction of light whilst conducting charge into the emission layer. Currently indium tin oxide (ITO) is the most commonly used TCE in OLEDs, as well as a host of applications such as organic photovoltaics (OPVs), displays and touch sensors. It has excellent sheet resistance (c. 15 Ω/□), high transmission in the visible wavelength range (typically 87% on average from 400 to 700 nm) and its fabrication process has been thoroughly optimised [1]. However, the cost of ITO is very high due to the scarcity of indium and the production process used to prepare the coatings. Indium migration has also been shown to limit the device lifetime [2,3]. Finally, ITO is also brittle, which is at odds with the mechanical flexibility of OLEDs [4] and other organic electronics.

Thus, there is a strong motivation to develop alternative TCEs to ITO [5–7]. TCEs in general must have a combination of high transmission at the emission wavelength and low sheet resistance. In addition, to lower the manufacturing cost and to allow new device architectures to be designed they should also be inexpensive and flexible. Conductive polymers such as poly(3,4-ethylenedioxythiophene): polystyrene sulfonate (PEDOT:PSS) [8,9], silver nanowires (AgNWs) [10,11], nanometre thin metal films [12], metal grids [13–16], carbon nanotubes (CNTs) [17–20], graphene [17] and graphene oxides [21] have all been proposed as alternative TCEs. Whilst they are all potentially viable solutions for replacing ITO in specialist applications, this paper focuses on the use of nanometre thin metal grids in polymer OLEDs.

The transmission and sheet resistance of thin metal grids as TCEs have been previously investigated [12,13],

* Corresponding author.
E-mail address: s.silva@surrey.ac.uk (S.R.P. Silva).

http://dx.doi.org/10.1016/j.orgel.2014.09.036
1566-1199/

and have been used to fabricate devices in proof of concept applications [14,22–25]. One of the advantages of metal grid TCEs is that their sheet resistance and transmission can be fine-tuned by adjusting the line width, spacing or thickness. For a given line width and line spacing, the transmission can be kept constant whilst the sheet resistance can be reduced by increasing the grid line thickness. It is suggested in the literature that thick metal lines (i.e. increasing perpendicular to the surface) will make the best metal grid-based devices as this minimises the sheet resistance, whilst the transmission is maintained at a high level. For example, Kuang et al. [16] reported a sheet resistance of 9.7 Ω/□ with a transmission of 80% using 1.2 μm thick parallel lines made of gold, and Galagan et al. [22] fabricated a 2 μm thick printed silver hexagonal grid which gave a sheet resistance of 1 Ω/□ with a metal coverage area of 8% (transmission was not specified, but it is presumed to be about 92%).

In this paper, we have investigated the performance of polymer OLEDs with respect to the line thickness of a silver grid TCE. Whilst many papers study the TCE in isolation and have made single devices (mostly OPVs) to demonstrate an application, there are no papers which study the variation in OLED performance with the metal grid thickness. Here we show that the perceived theory that thicker grids are optimal may actually be incorrect, with the better optimised device having a higher sheet resistance TCE than some of the other OLEDs.

2. Experimental methods

Silver hexagonal grids were fabricated by photolithography on a transparent 15 mm × 15 mm × 0.7 mm glass substrate. The photolithography process is described in the Supplementary Materials. Two masks with different hexagonal grid dimensions were used: one mask with 2 μm line width and 60 μm line spacing and the other with 3 μm line width and 10 μm line spacing. The silver grids produced from the two masks therefore had different sheet resistance and light transmission for a given grid line thickness. The grid line thickness was measured by AFM (Atomic Force Microscopy, Veeco Dimension 3100) after the lift-off process.

Silver grid TCEs of up to 40 nm line thickness can be used to make OLEDs as the surface was smooth enough and could be sufficiently planarised by a single layer of PEDOT:PSS. To make thicker grid lines, the grid fabrication method had to be adjusted. There have been reports in the literature of groups maintaining a smooth surface whilst using very thick grid lines [22], but they have not disclosed the method of planarisation. A simple approach would be to use a very thick layer of PEDOT:PSS, but that would be detrimental to the OLED performance. Therefore, we derived our own method of planarisation, with the aim of demonstrating the performance of OLEDs using a 100 nm thick silver grid TCE. There are a number of other routes that could be used to embed the grids in the substrate. The results surprisingly show that thick grid TCEs do not make the best OLEDs, so the concept of having to embed the grid lines may not be required.

The method used to make 100 nm thick grid lines for TCEs was the same as for making grid lines less than 40 nm thick, except that the lift-off resist PMGI SF6 (see Supplementary Materials) was not used and an extra step was inserted. After patterning the S1805 photoresist, it was hard baked for 2 h at 90 °C on a hotplate before etching the glass substrate for 1 min in buffered hydrofluoric acid (HF) diluted with deionised (DI) water in a 5:1 (DI water: HF) ratio. The result was troughs about 100 nm deep etched in the glass in which silver could be deposited in the required hexagonal grid pattern. Depositing 100 nm of silver through the openings in the photoresist therefore resulted in a flat TCE surface. Up to an extra 40 nm of silver protruding above the surface can be allowed before the device is short-circuited. The photoresist was then removed by leaving it in acetone overnight. Using this method, a 111 nm thick large spacing silver grid was produced for an OLED in this paper. The etched depth of the glass was 87 nm, and 24 nm of the silver lines were above the glass surface.

The TCE substrates were cleaned by sonicating for 10 min in acetone, isopropanol and methanol and were then blown dry with nitrogen. They were not plasma ashed as this damages the surface of the silver grid lines. Therefore, to maintain the same fabrication conditions for an accurate comparison, the ITO substrate was not plasma ashed either. This meant that the PEDOT:PSS does not wet as well to the TCE surface as it would if it was plasma ashed. However, after spin coating PEDOT:PSS outside the glovebox at a speed of 3000 rpm for 1 min with an acceleration of 330 rpm/s, it was observed that a uniform thin film is formed on the surface of both the silver grid and the ITO.

The remaining deposition steps were performed inside a nitrogen filled glove box. After depositing PEDOT:PSS (Clevios PVP AI 4083, Heraeus, Germany), the substrate was annealed on a hotplate at 150 °C for 10 min. Poly[(9,9-dioctylfluorenyl-2,7-diyl)-co-(4,4′-(N-(p-butylphenyl))diphenylamine)] (TFB) (ADS 259BE, American Dye Source) was then spin coated at 2000 rpm for 1 min at maximum acceleration (30,000 rpm/s). The substrate was baked again at 150 °C for 10 min. Poly[(9,9-di-n-octylfluorenyl-2,7-diyl)-alt-(benzo[2,1,3]thiadiazol-4,8-diyl)] F8BT (ADS 133YE, American Dye Source) was spin coated on the substrate at 1000 rpm for 1 min with an acceleration of 330 rpm/s, followed by a further anneal of 10 min at 150 °C. A mask was used to define the aluminium electrodes on the substrate. The mask (with the substrate) was placed inside an evaporator and 2,9-dimethyl-4,7-diphenyl-1,10-phenanthroline BCP (5 nm) and aluminium (60 nm) were evaporated on to the substrate. The OLED was encapsulated using a UV-light cure adhesive (Loctite 3491) and a small piece of microscope glass slide to protect the organic layers from oxygen and water. The active area of the OLED was 8 mm^2.

3. Results

3.1. Silver grid TCE characterisation

The transmission of each grid TCE was measured prior to making OLEDs on them (Fig. 1(a) and (b)). The variation

in transmission is due to small imperfections in the photolithography process. For the large spacing silver grid, the standard deviation is about ±0.5%, whilst for the small spacing grid, it is about ±5%. From the AFM height images taken of the grids, it could be observed that the grid line width is at times wider (by < 1 μm) than the mask line width. For the large spacing grid, this has a smaller effect (1/60th) than for the small spacing grid (1/10th). Therefore, the standard deviation in the transmission of the small spacing grid is greater than for the large spacing grid.

For sheet resistance measurements, silver grids were fabricated on microscope glass slides and the Transfer Length Method (TLM) [26] was used (Fig. 1(c) and (d)). For the large spacing silver grid, the sheet resistance was 200 Ω/□ for a 10 nm line thickness, and dropped to 25 Ω/□ for a 40 nm line thickness. With a transmission of 94% at a wavelength of 550 nm, the large spacing grid with 40 nm line thickness had properties comparable to ITO (a sheet resistance of 15 Ω/□ and transmission of 99% at 550 nm and 87% on average from 400 to 700 nm). For the small spacing silver grid, the sheet resistance reduced from 30 Ω/□ for a 10 nm line thickness to 7 Ω/□ for a 40 nm line thickness.

3.2. OLED luminance and current density

3.2.1. Large spacing silver grid TCE OLEDs

Polymer OLEDs were made consisting of the following layers: TCE (silver (Ag) grid or ITO)/PEDOT:PSS/TFB/F8BT/BCP/aluminium (Fig. 2).

It is generally expected that as sheet resistance decreases, more charges can be injected into the emission layer and the luminance would increase for a given voltage. In our experiments, it appears that as the line thickness increases and the sheet resistance decreases, the luminance does not show a significant change. The exception is the 21 nm OLED which has the highest luminance (7100 cd/m^2) of the OLEDs measured in this set (Fig. 3). The maximum luminance of the other large spacing grid OLEDs range from 4800 to 5400 cd/m^2. Nevertheless, all these OLEDs have a luminance lower than the maximum luminance of an ITO OLED (22,700 cd/m^2).

In the OLED structure used here, the layer which conducts holes across the gaps in the grid TCE (and into the emission layer) is PEDOT:PSS, but it has a high sheet resistance on the order of 10^8 Ω/□ at a thickness of 30 nm. Therefore, holes can only move a short distance horizontally, away from the grid lines, before recombining with electrons in the emission layer. This means that only a small area determined by the diffusion length of the holes from the grid lines will emit light (Fig. 4 and Table 1). The active regions are small and there are large dark spaces. Decreasing the sheet resistance of the grid will only serve to pump more holes into this area (close to the gridlines) but not much beyond it. Therefore, it will increase the luminance for a given voltage in this active volume only. However, this will not increase the efficiency of the device. It might even decrease the efficiency as the current density in the emitting F8BT layer will reach very high levels for a given luminance and might damage the polymer layers or cause exciton quenching.

The optical transmission of the silver grid lines also decreases as the grid line thickness increases. For example, a 20 nm thick continuous silver film has a transmission of 22%, whereas a 40 nm thick silver film allows only 5% of light through and no light at all passes through a 111 nm thick silver film [27]. Whilst the transmission of the silver grid as a whole varies from 97% to 94%, the transmission of the grid lines themselves decreases by a greater quantity. The small increase in luminance due to more current injection at a given voltage will not compensate for the decrease in transmission of the grid lines. Only a small area around the grid lines emits light and for very thick grid lines, the luminance from directly beneath the grid lines is obscured. When the grid lines are thinner, some light can actually pass through them.

This is illustrated in the series of light microscope images in Fig. 4. In Fig. 4(a) the line thickness is 21 nm and the grid line cannot be observed. In Fig. 4(c) the grid line thickness is 39 nm and the shadow of the grid line is

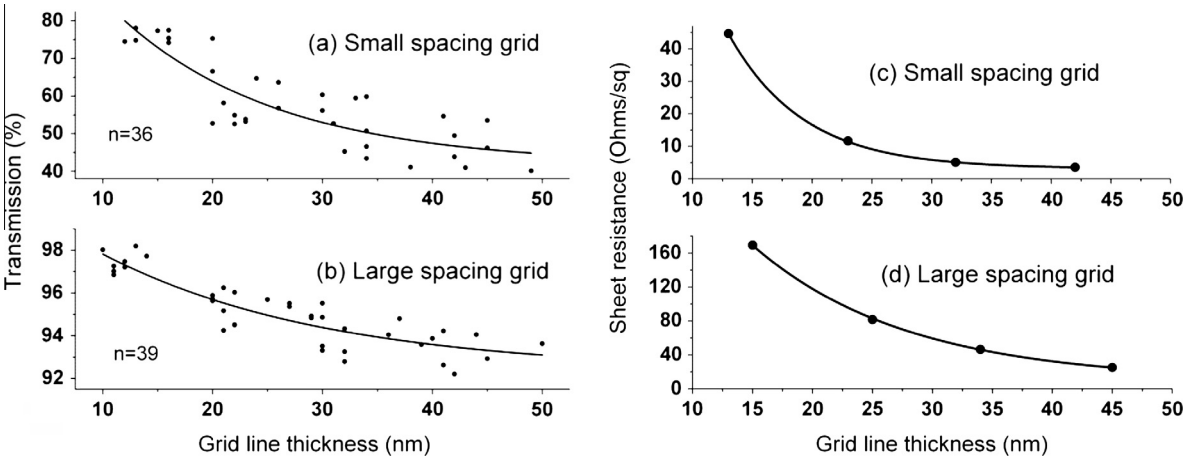

Fig. 1. Transmission at 550 nm wavelength of (a) small spacing and (b) large spacing silver grids (n = number of data points); and sheet resistance of (c) small spacing and (d) large spacing silver grids. The solid black line is the best-fit for the measurement data points.

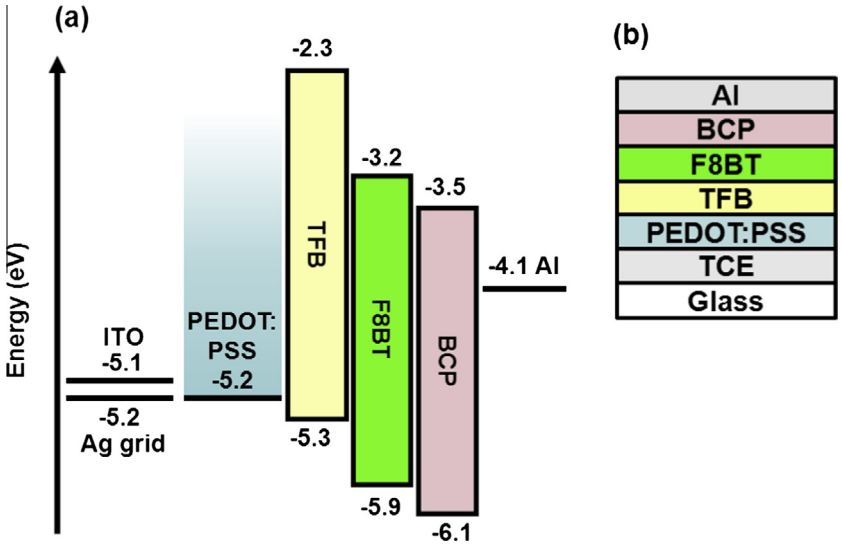

Fig. 2. (a) OLED energy levels of the constituent materials and (b) the cross section of the proposed OLED architecture. Both diagrams are not to scale.

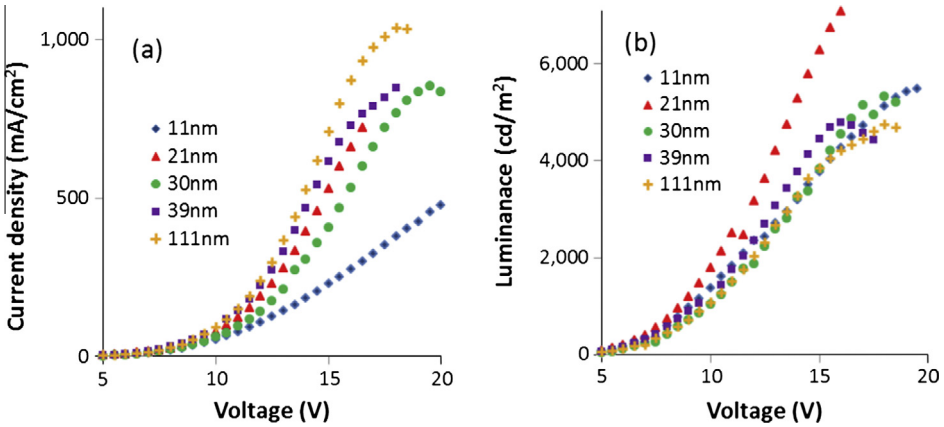

Fig. 3. (a) *J–V* and (b) luminance characteristics of OLEDs based on large spacing silver grids (60 μm line spacing, 2 μm line width) of different thicknesses (11–111 nm).

clearly visible. It is blocking the light and this could be the reason for the poorer luminance and efficiency of the OLEDs with thicker grid lines. Fig. 4(b) shows the progressive appearance of the grid line shadow at an intermediate line thickness (30 nm). Fig. 4(d) is an OLED using a 111 nm grid line thickness and it can be seen that the grid line is even darker as it blocks the light completely. Fig. 5 is a light intensity profile taken perpendicular to a grid line in the OLED in Fig. 4. It shows subjectively the blocking of the light by the grid line with the increase in the grid line thickness. Table 1 gives the FWHM (full-width at half-maximum) of the silver grid OLED emission intensity in Fig. 5. This is a route to estimating the distance from the grid lines that the holes drift before recombining in the emission layer with electrons as a function of carrier diffusion mobility and electric field induced charge transport.

The data suggests that the assumption made in previous research that using a very thick grid line, sometimes up to 2 μm, will make the best transparent conducting grid and increase the luminance of the OLED, is incorrect. The global sheet resistance of a thick grid TCE might reach a very low value, but the local sheet resistance must also be considered. As the sheet resistance of the transparent conducting grid begins to level off with increasing thickness, it is no longer the limiting factor of the OLED performance. The sheet resistance of the material or polymer between the grid lines (in the gaps) is then the new limiting factor that must be improved. This means that a more conductive polymer must be used e.g. PEDOT:PSS PH1000 which has a sheet resistance of 200 Ω/□ and a transmission of 97% (versus 10^8 Ω/□ and 97% for PEDOT:PSS Al4083 films of equivalent thicknesses (30 nm)), CNTs [28,29], or graphene [30], which in theory have an even lower sheet resistance. Alternatively, the line spacing can be reduced. Our results also suggests that a grid line thickness of up to 40 nm may be sufficient for metal grid TCE OLEDs and methods of planarising the grid surface might not be necessary.

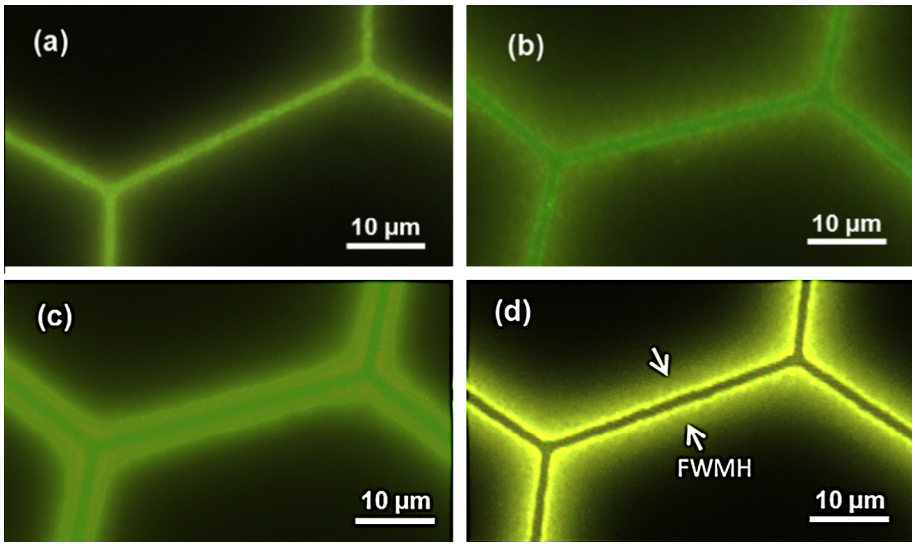

Fig. 4. Light microscope images of light emission from the OLED through large spacing silver grids of (a) 21 nm, (b) 30 nm, (c) 39 nm, (d) 111 nm thicknesses, as the transparent anode. As an example, the FWHM of the light intensity reported in Table 1 is shown in (d). The lamp of the microscope is turned off. The only light that is captured is from the OLED emission.

Table 1
FWHM (Full-width at half-maximum) of silver grid OLED emission intensity in Fig. 5.

Grid thickness (nm)	FWHM (a.u.)	FWHM (μm)
21	0.84	7 ± 1
30	1.7	14 ± 1
39	1.38	11 ± 1
111	0.85	7 ± 1

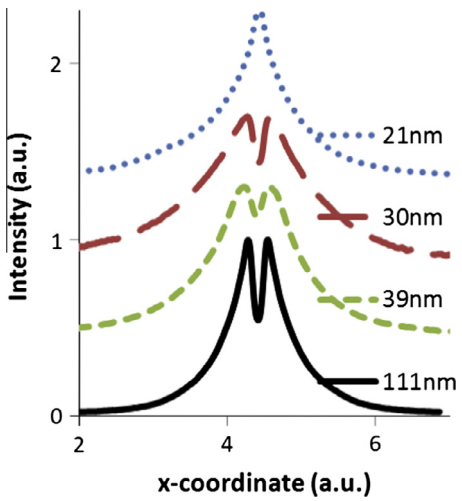

Fig. 5. Light intensity profile across a grid line in a large spacing silver grid TCE OLED during operation showing the light being blocked by the grid line. The *x* coordinate is at right angles to the grid line. ImageJ was used for the data analysis.

3.2.2. Small spacing silver grid TCE OLEDs

According to Table 1, the furthest distance from a grid line from which light is emitted (as represented by half the FWHM) was about 6 μm [=(14–2)/2]. For there to be no dark spaces in the emission of the OLED, the line spacing of an improved hexagonal grid TCE had to be at most twice this distance. Since holes can reach the middle of the gaps in the grid from two opposite conducting grid lines, this means that no spot is further away from a grid line than the maximum distance the holes can travel and that all the available area of F8BT can emit light. Therefore, a small spacing silver grid with a line spacing of 10 μm and a line width of 3 μm was used. The small spacing grid mask was borrowed from another experiment, and the line spacing was slightly smaller than the estimated hole diffusion length. This is not a problem as there is a small uncertainty in the FWHM estimation and a grid with this line spacing would be certain of having no dark areas when the OLED was in operation. This was successfully achieved as shown by the light microscope photographs in Fig. 6. In Fig. 6(b), the luminance from the gaps and through the grid lines are the same intensity, which makes it difficult to distinguish the grid lines. When the grid line is thicker as in Fig. 6(c), the grid lines obscure some of the emission and the shadow of the grid lines can be seen. Nevertheless, there are no dark areas in the gaps between the grid lines. This is in agreement with the prediction based on our previous analysis of the diffusion length of carriers before emissive recombination. At lower magnification, light emission can be seen to be uniform across the entirety of the 8 mm^2 OLED pixels (Fig. 6(d)).

OLEDs with the small spacing silver grids performed better than OLEDs with the larger spacing silver grids (Fig. 7). This is despite their lower transmission (64% for a 20 nm grid line thickness) due to the smaller line spacing. The turn-on voltage is the same as the reference ITO OLED (3.0 V). The luminance of the 20 nm thick small spacing silver grid OLED is close to that of an ITO OLED which has a much higher transmission (99% at 550 nm). The maximum

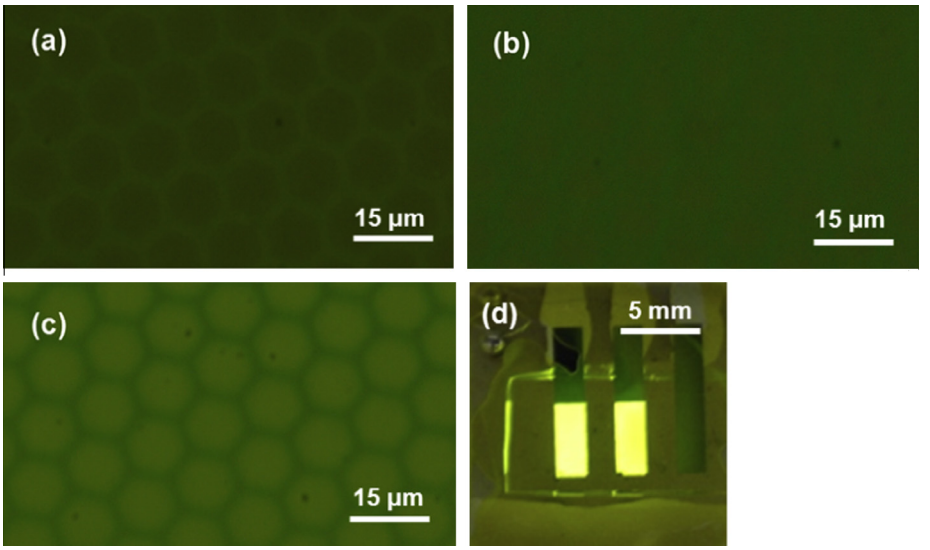

Fig. 6. Light microscope images of OLED light emission through small spacing silver grids of (a) 20 nm, (b) 30 nm, and (c) 40 nm thicknesses as the transparent anode. The gaps between the grid lines emit light uniformly. (d) Photograph of two operating OLED pixels demonstrating the uniformity of light emission.

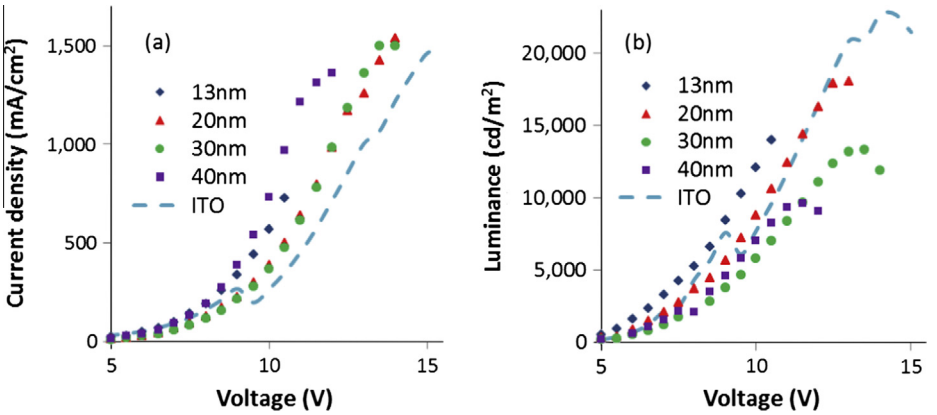

Fig. 7. (a) *J–V* and (b) luminance characteristics of OLEDs based on small spacing silver grids (10 μm line spacing, 3 μm line width) of different thicknesses. The data for the reference ITO OLED is also included for comparison (the *J–V* curves for the 20 nm and 30 nm thick grid TCE OLEDs overlap, so they may be difficult to see).

luminance of the ITO OLED is 22,700 cd/m^2 which occurs at 14.5 V, whereas the maximum luminance of the 20 nm thick small spacing silver grid OLEDs is 18,100 cd/m^2 and occurs at 13.0 V. This is 80% of the luminance of the ITO OLED (Table 2). In contrast, the transmission of the 20 nm thick silver grid TCE is 65% of the transmission of ITO at 550 nm wavelength. If the silver grid was simply blocking the light, then the maximum luminance of the grid TCE OLED should be 65% of the maximum luminance of the ITO OLED, and not 80%. The comparison may also be examined by adjusting (or normalising) the luminance of the grid OLEDs according to the difference in transmission compared to ITO using the following equation:

$$\textit{Adjusted 'Normalised' Luminance} = \frac{\textit{Grid OLED Max. Luminance}}{\textit{Grid transmission}} \times \textit{ITO transmission} \qquad (1)$$

This gives an idea of what the maximum luminance could be if the grid TCE had the same transmission as ITO, assuming the sheet resistances are identical (Table 2). It allows a further variable for the optimising of the light output when it comes to the design of OLEDs. The sheet resistance, of course, increases as the grid line thickness decreases, but the 20 nm thick small spacing grid had a sheet resistance of 16 Ω/□ which is almost the same as ITO (15 Ω/□). The results of the calculations show that the 20 nm thick silver grid OLED has an adjusted "normalised" luminance of almost 28,000 cd/m^2 which is higher than the ITO OLED. These comparisons indicate that there is an effect in the silver grid TCE that either increases the light emission in the polymer layer or improves the outcoupling of light and is not present in ITO. This will be investigated in future work.

The highest luminance of the large spacing silver grid was achieved with a 21 nm thick grid (7100 cd/m^2 at

Table 2
Maximum luminance of small spacing silver grid TCE OLEDs of different thicknesses, adjusted according to the difference in transmission compared to ITO.

Grid line thickness (nm)	Transmission at 550 nm (%)	Percentage of ITO transmission (%)	Percentage of ITO luminance (%)	Maximum luminance (cd/m^2)	Adjusted luminance (cd/m^2)
13	71.8	72.5	66.3	15,044	20,743
20	64.4	65.1	79.7	18,063	27,767
30	58.8	59.4	58.7	13,321	22,428
40	56.1	56.7	42.4	9620	16,977
ITO	99	100	100	22,675	22,675

Table 3
Voltage required for luminance of 100 and 1000 cd/m^2 for the large (L) and small (S) spacing silver grid and the reference ITO (in bold) TCE OLEDs.

Grid line thickness (nm)	Voltage at 100 cd/m^2 (V)	Voltage at 1000 cd/m^2 (V)
11 (L)	5.5	9.1
21 (L)	5.4	8.6
30 (L)	5.9	9.9
39 (L)	5.5	9.2
111 (L)	5.9	9.8
ITO	**4.6**	**6.4**
13 (S)	4.2	5.5
20 (S)	4.3	6.1
30 (S)	4.6	6.8
40 (S)	4.6	6.4

16.0 V). The turn-on voltage was also 3.0 V. It appears that regardless of the line spacing of the silver grid TCE, the highest luminance is achieved for a grid line thickness of about 20 nm and not for the thickest grid line, contrary to expectation.

Higher voltages are required to operate the large spacing grid OLEDs at 100 and 1000 cd/m^2 (typical luminances of display screens and room lighting) than for ITO (Table 3), but for the small spacing grid OLEDs they have the same brightness at similar voltages to ITO. There does not appear to be any correlation between the current density of the OLED below the turn-on voltage (or leakage current) and the voltage required to operate the OLED at 100 and 1000 cd/m^2. There is very little leakage current in all the OLEDs (Supplementary Materials, Fig. S1(a) and (b)). The 13 nm and 20 nm thick small spacing grids have lower operating voltages than ITO for these luminances. This shows that even though the small spacing grids have lower transmission than ITO, at low voltages, the small spacing grid OLEDs have higher luminance than the reference ITO OLED. This highlights the potential for replacing ITO with grid TCEs in OLEDs.

The work functions of the silver grids were measured (Ambient Single Point Kelvin Probe, Anfatec, Germany) to be between −5.1 and −5.3 eV for different spacings and thicknesses. No trend was apparent when the grid spacing or thickness was changed. The work function of solvent cleaned (non-plasma ashed) ITO was measured to be −5.1 eV. After oxygen plasma ashing, the ITO work function increased to −5.7 eV. This is similar to the results reported in [31]. Consequently, the silver grid TCEs had similar work functions to the reference ITO TCE, and as a result, the hole injection barrier is expected to be similar in all the OLEDs. In accordance with the similar work functions of the TCEs, all the OLED turn-on voltages (defined as the voltage at which a luminance of 1 cd/m^2 is reached) are equivalent at 3.0 V (Supplementary Materials, Fig. S1(c) and (d)).

3.3. Luminous efficiency

The luminous efficiencies of the OLEDs with a silver grid TCE are comparable to the reference ITO OLED. The luminous efficiency of the silver grid OLED decreases as the grid line thickness increases. This supports the argument that thicker grid lines are not necessarily the best option. The best large spacing silver grid OLED (11 nm) has a maximum luminous efficiency (9.6 cd/A) similar to the ITO OLED (9.8 cd/A), although the peak occurs at a lower operating voltage (6.0 V as opposed to 9.5 V) (Fig. 8(a)). In addition, the best small spacing silver grid OLED (13 nm) has a higher efficiency at lower operating voltage (11.3 cd/A at 6.0 V) than the ITO OLED (Fig. 8(b)).

The luminous efficiency of the ITO OLED only peaks within a short operating voltage range. For example, it is above 5 cd/A from 6 V to 14 V. In contrast, the luminous efficiency of the 21 nm thick large spacing silver grid OLEDs is higher than 5 cd/A from 4 V to 16 V. At low voltages (4 V to 6 V), all the silver grid OLEDs are more efficient than the ITO OLED. At 5 V, the 20 nm thick small spacing silver grid OLED has a luminance of 318 cd/m^2, whilst the ITO OLED has a luminance of 282 cd/m^2. Therefore, the silver grid OLED emits a similar level of light as the ITO OLED, but at a higher efficiency. This can be beneficial for prolonging the lifetime of the silver grid OLEDs, as they can be operated at a lower voltage.

It appears that the OLEDs burn out at current densities close to 1000 mA/cm^2 for the large spacing grid OLEDs, and 1500 mA/cm^2 for the small spacing grid and ITO OLEDs. The ITO used in these experiments has a lower sheet resistance than the large silver grid TCE. Therefore, the ITO OLEDs reach a higher current density and fail at a lower voltage. This might be the reason why they would appear to operate at high efficiency over a shorter voltage range than the large spacing silver grid OLEDs. In fact, the small spacing grid TCE has a similar sheet resistance to ITO, and OLEDs made with this TCE have a similar luminous efficiency range as the ITO OLEDs.

The large spacing grid OLEDs reach a lower current density than the small spacing grid OLEDs before failing. The current density is calculated over the whole OLED area, but the local current density on the large spacing grid lines is higher, whereas for the small spacing grid OLEDs it is spread out over a larger area. Therefore, the current

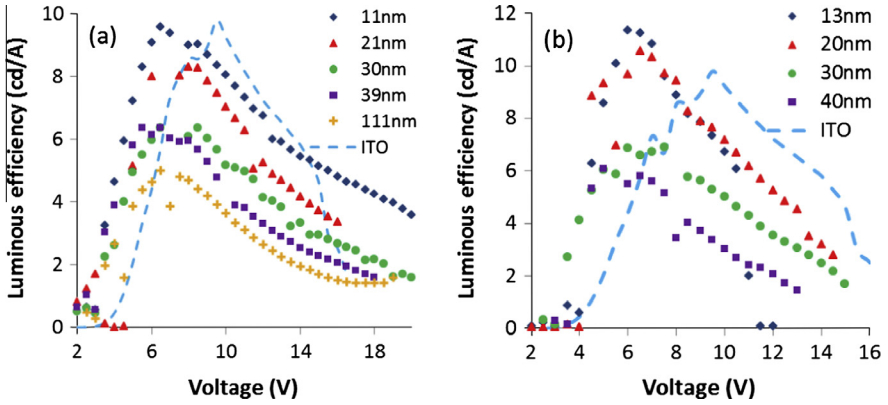

Fig. 8. (a) Large spacing silver grid (60 μm, 2 μm) and (b) small spacing silver grid (10 μm, 3 μm) OLED luminous efficiency compared to ITO.

density on the grid line may be the same in both OLEDs at the point of failure, but as the current density is more concentrated in the large spacing grids, the overall OLED current density is different.

The high current density and voltage can cause the OLED to fail due to the electrochemical migration of silver from the grid TCEs, or indium from ITO, leading to the growth of dendrites between the two electrodes and short circuiting of the device. This issue has been reported in the literature between solder points on circuit boards [32–34], but not in OLEDs or OPVs. However, under very extreme conditions (e.g. above 150 °C, 90% relative humidity, and 20 V to 90 V), this could be a problem in OLEDs. One way to solve this problem is to use an alloy, e.g. 70% silver: 30% palladium [35], or to encapsulate the OLED as was done here, as water is a critical ingredient for electrochemical migration. The short-circuit can also be reversed to an extent (but not completely) by applying a reverse bias to the OLED for a short time [2,36]. This might cause the ions to migrate back in the other direction, and could be why electrochemical migration is not observed under alternating current. Nevertheless, the more likely causes of failure in OLEDs are the formation of pin holes, non-uniform thin films or polymer degradation [2,3]. These problems can be avoided by better film formation, fabrication in a clean room to minimise dust particles causing shorts, or by encapsulating the OLED to prevent polymer degradation.

One area which can be improved is the luminance of the silver grids which is not as high as the ITO OLED, even though they are more efficient. For the large spacing silver grids, the main reason is that the sheet resistance of the grid is higher than ITO, and therefore less current can be pumped into the active layer. This would result in less recombination of electrons and holes, and therefore less photon emission at a given voltage than the ITO OLED. For the small spacing silver grids, the transmission is lower than for ITO since the silver grid TCE blocks more light, and this limits the luminance.

Even more importantly, as can be seen in Fig. 4, there are gaps in the large spacing silver grid TCE where no photons are emitted. Only a fraction the F8BT active layer is being used to create photons and this is inefficient. If the large spacing silver grid OLEDs have comparable efficiency to ITO OLEDs and yet do not use all the available area of F8BT to emit light, then this suggests that if current could be conducted to those gaps in the grid [37] and the transmission is kept above 90%, then the silver grid OLEDs will have a higher luminance and potentially higher efficiency. The gaps in the small spacing silver grid are already illuminating, so they cannot be improved by this method.

4. Conclusion

All the data collected from the silver grid OLEDs fabricated in this paper indicate that very thick grid lines will not necessarily make the best performing OLEDs. The OLEDs which use silver grids with line thicknesses of 10–20 nm as the TCE had higher maximum luminance and luminous efficiency than OLEDs with thicker grid lines. The best devices with silver grids had better luminous efficiency than ITO OLEDs, particularly at low voltages. Although the efficiency is high, the maximum luminance can be further improved. The large spacing grid has more potential for improvement than the small spacing grid OLED. There are dark areas in the gaps between the grid lines. If charge is conducted to those areas perhaps by using CNTs, graphene, AgNW or conductive PEDOT:PSS, the luminance is expected to be higher since the transmission will remain above 90% and the whole area of F8BT will be used to its full potential.

Acknowledgement

The authors would like to acknowledge the support received from the EU FP7 program SMARTONICS (grant agreement number 310229).

Appendix A. Supplementary material

Supplementary data associated with this article can be found, in the online version, at http://dx.doi.org/10.1016/j.orgel.2014.09.036.

References

[1] H. Kim, C.M. Gilmore, A. Pique, J.S. Horwitz, H. Mattoussi, H. Murata, Z.H. Kafafi, D.B. Chrisey, J. Appl. Phys. 86 (1999) 6451.
[2] J.R. Sheats, D.B. Roitman, Synth. Met. 95 (1998) 79.

[3] H. Aziz, Z.D. Popovic, Chem. Mater. 16 (2004) 4522.
[4] R. Paetzold, K. Heuser, D. Henseler, S. Roeger, G. Wittmann, A. Winnacker, Appl. Phys. Lett. 82 (2003) 3342.
[5] K. Ellmer, Nat. Photon. 6 (2012) 809.
[6] L. Hu, H. Wu, Y. Cui, MRS Bull. 36 (2011) 760.
[7] J. Cui, A. Wang, N.L. Edleman, J. Ni, P. Lee, N.R. Armstrong, T.J. Marks, Adv. Mater. 13 (2001) 1476.
[8] S.K. Hau, H.-L. Yip, J. Zou, A.K.-Y. Jen, Org. Electron. 10 (2009) 1401.
[9] A.S. Alshammari, M. Shkunov, S.R.P. Silva, Phys. Stat. Sol. RRL 8 (2014) 150.
[10] S. De, T.M. Higgins, P.E. Lyons, E.M. Doherty, P.N. Nirmalraj, W.J. Blau, J.J. Boland, J.N. Coleman, ACS Nano 3 (2009) 1767.
[11] J.-Y. Lee, S.T. Connor, Y. Cui, P. Peumans, Nano Lett. 8 (2008) 689.
[12] D.S. Ghosh, T.L. Chen, V. Pruneri, Appl. Phys. Lett. 96 (2010) 041109.
[13] A. Cheknane, Prog. Photovolt. 19 (2011) 155.
[14] K. Tvingstedt, O. Inganas, Adv. Mater. 19 (2007) 2893.
[15] W. Kubo, S. Fujikawa, J. Mater. Chem. 19 (2009) 2154.
[16] P. Kuang, J.-M. Park, W. Leung, R.C. Mahadevapuram, K.S. Nalwa, T.-G. Kim, S. Chaudhary, K.-M. Ho, K. Constant, Adv. Mater. 23 (2011) 2469.
[17] Z. Wu, Z. Chen, X. Du, J.M. Logan, J. Sippel, M. Nikolou, K. Kamaras, J.R. Reynolds, D.B. Tanner, A.F. Hebard, A.G. Rinzler, Science 305 (2004) 1273.
[18] A. Inigo, J. Underwood, S.R.P. Silva, Carbon 49 (2011) 4211.
[19] S. Shi, S.R.P. Silva, Carbon 50 (2012) 4163.
[20] G.D.M.R. Dabera, K.D.G.I. Jayawardena, M.R.R. Prabhath, I. Yahya, Y.Y. Tan, N.A. Nismy, H. Shiozawa, M. Sauer, G. Ruiz-Soria, P. Ayala, V. Stolojan, A.A.D.T. Adikaari, P.D. Jarowski, T. Pichler, S.R.P. Silva, ACS Nano 7 (2013) 556.
[21] S. Shi, V. Sadhu, R. Moubah, G. Schmerber, Q. Bao, S.R.P. Silva, J. Mater. Chem. C 1 (2013) 1708.
[22] Y. Galagan, J.-E.J. Rubingh, R. Andriessen, C.-C. Fan, P.W. Blom, S.C. Veenstra, J.M. Kroon, Sol. Energy Mater. Sol. Cells 95 (2011) 1339.
[23] M.-G. Kang, M.-S. Kim, J. Kim, L.J. Guo, Adv. Mater. 20 (2008) 4408.
[24] J.-S. Yu, I. Kim, J.-S. Kim, J. Jo, T.T. Larsen-Olsen, R.R. Sondergaard, M. Hosel, D. Angmo, M. Jorgensen, F.C. Krebs, Nanoscale 4 (2012) 6032.
[25] F.L.M. Sam, C.A. Mills, L.J. Rozanski, S.R.P. Silva, Laser Photon. Rev. 8 (2014) 172.
[26] D.K. Schroder, Semiconductor Material and Device Characterization, second ed., Wiley-Interscience, New York, USA, 1998.
[27] E.D. Palik, Handbook of Optical Constants of Solids, Academic Press, Florida, USA, 1985.
[28] D.S. Hecht, L. Hu, G. Grüner, Curr. Appl. Phys. 7 (2007) 60.
[29] D.S. Hecht, L. Hu, G. Irvin, Adv. Mater. 23 (2011) 1482.
[30] Y. Zhu, Z. Sun, Z. Yan, Z. Jin, J.M. Tour, ACS Nano 5 (2011) 6472.
[31] K. Furukawa, Y. Terasaka, H. Ueda, M. Matsumura, Synt. Met. 91 (1997) 99.
[32] S. Yang, A. Christou, IEEE Trans. Dev. Mater. Rel. 7 (2007) 188.
[33] T. Takemoto, R. Latanision, T. Eagar, A. Matsunawa, Corros. Sci. 39 (1997) 1415.
[34] S. Krumbein, IEEE Trans. Compon. Hybrids Manuf. Technol. 11 (1988) 5.
[35] J. Lin, J. Chan, Mater. Chem. Phys. 43 (1996) 256.
[36] Z.D. Popovic, H. Aziz, IEEE J. Sel. Topics Quantum Electron. 8 (2002) 362.
[37] F.L.M. Sam, G.D.M.R. Dabera, K.T. Lai, C.A. Mills, L.J. Rozanski, S.R.P. Silva, Nanotechnology 25 (2014) 345202.